

Comparison of feedback linearization and flatness control for anti-slip regulation (ASR) of an hybrid vehicle: From theory to experimental results

Cédric Chapuis, Eric Bideaux, Xavier Brun, Nicoleta Minoiu

▶ **To cite this version:**

Cédric Chapuis, Eric Bideaux, Xavier Brun, Nicoleta Minoiu. Comparison of feedback linearization and flatness control for anti-slip regulation (ASR) of an hybrid vehicle: From theory to experimental results. European Control Conference (ECC), Jul 2013, Zürich, Switzerland. pp.446 - 451, 10.23919/ECC.2013.6669127 . hal-00988572

HAL Id: hal-00988572
https://hal.science/hal-00988572

Submitted on 17 Apr 2019

HAL is a multi-disciplinary open access archive for the deposit and dissemination of scientific research documents, whether they are published or not. The documents may come from teaching and research institutions in France or abroad, or from public or private research centers.

L'archive ouverte pluridisciplinaire **HAL**, est destinée au dépôt et à la diffusion de documents scientifiques de niveau recherche, publiés ou non, émanant des établissements d'enseignement et de recherche français ou étrangers, des laboratoires publics ou privés.

Copyright

Comparison of Feedback Linearization and Flatness Control for Anti-Slip Regulation (ASR) of an Hybrid Vehicle : From Theory to Experimental Results

Cedric Chapuis, Eric Bideaux, Xavier Brun and Nicoleta Minoiu-Enache

***Abstract*— This paper compares 3 ASR[1] control laws, a PI controller, a linearizing feedback and a flatness based control. First, the controllers are designed based on a two state equations vehicle model. Then, the controllers are experimentally validated on an hybrid vehicle (VELROUE) with rear electric wheels and front axle ICE[2] traction. Finally, the nonlinear control laws are compared to the PI controller that is classically used in the automotive industry.**

I. INTRODUCTION

The number of hybrid and electric vehicles has increased due to technical progress in the battery field and the strengthening of ecological norms. The hybrid technology leads to the multiplication of power sources in powertrain architectures and offers new opportunities for the control of vehicles chassis dynamics. In this paper, we will consider the ASR using different control theories. A PI controller, a linearizing feedback and a flat control law are tuned on a VELROUE prototype vehicle. VELROUE is a collaborative project subsidized by FEEMA which gathers RENAULT, MICHELIN and IFP. VELROUE's demonstrator (Fig. 1) is a bi-mode powered utility vehicle with an ICE driving the front wheels and two electric motors developed by MICHELIN, clutched to both rear wheels. The developed ASR functions will be here applied to control the rear wheels slip.

VELROUE rear wheels slip is controlled by commanding the torques from the electric motors. [1] implements an ASR function using for instance a linear PID controller fed by the difference between the targeted and the measured slipping. The wheel-road contact force is computed thanks to a vehicle model similar to the model (1) used later in this paper and a real time differentiation of the rotating wheel speed. Not only PID control, but also several techniques based on nonlinear control have been applied to do anti-slip regulation. A Model Following Control was used by [2] and [3]. First order sliding mode controllers were synthesized by [4], [5] and [6]. This control technique was also applied by [4] on a vehicle on rail. The sliding surface in these approaches is defined by the difference between the desired and the measured absolute slipping. This sliding mode control was applied by [5] on a vehicle with a wheel-road contact model based on the LuGre model developed in [7]. The difference with the previous papers is that the sliding surface in [6] is defined by the difference between the desired and the measured slipping ratio. For a function similar with the ASR that controls also the slip, the ABS[3], a fuzzy logic control was introduced by [8] and a genetic algorithm was used to determine in real time the large number of tuning parameters required by the fuzzy logic controller. Two fuzzy controllers were also compared to a linearizing feedback control by the authors in [8]. [9] proposed the linearizing feedback control for the ASR function.

This short review of the literature shows that ASR control laws have been developed for ICE and electric vehicles. In our work the novelty consists in a comparison of a PI controller, a linearizing feedback and a flatness control, which are applied to an innovative architecture of hybrid vehicle. These controllers are developed to control the slipping of the rear wheels driven by two independent electric motors.

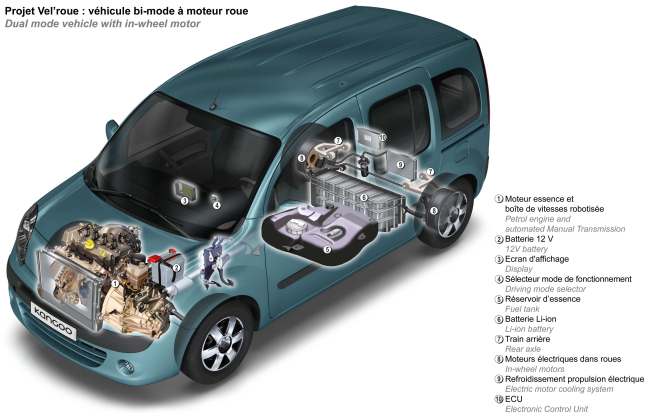


Fig. 1. VELROUE demonstrator vehicle

This work was supported by ANRT (CIFRE 10/169) in collaboration with RENAULT and the AMPERE LAB.

C. Chapuis is a PhD student in the Automatic Control and Mechatronic Team at Ampere Lab UMR CNRS 5005 and in the Vehicle Control Team at Renault SAS Research and Advanced Engineering Department, Renault SAS, 1 avenue du Golf, 78288 Guyancourt, France chapuis.cedric@gmail.com

Dr E. Bideaux is Professor at Ampere Lab UMR CNRS 5005 and head of Methods of System Engineering Department, 25 avenue Jean Capelle, F-69621 Villeurbanne Cedex, France eric.bideaux@insa-lyon.fr

Dr X. Brun is Professor at Ampere Lab UMR CNRS 5005 and head of Automatic Control and Mechatronic Team, 25 avenue Jean Capelle, F-69621 Villeurbanne Cedex, France xavier.brun@insa-lyon.fr

Dr N. Minoiu-Enache is a research engineer in the Vehicle Control Team at Renault SAS Research and Advanced Engineering Department, Renault SAS, 1 avenue du Golf, 78288 Guyancourt, France nicoleta.minoiu-enache@renault.com

[1] Anti-Slip Regulation

[2] Internal Combustion Engine

[3] AntiBlockierSystem

First the vehicle model used for the synthesis of the nonlinear controllers is described in section 2. The linearizing feedback and the flat control laws are then synthesized. Experimental validation results are presented in section 3 before concluding in section IV.

II. VEHICLE MODEL AND CONTROL LAWS SYNTHESIS

A. Vehicle Model

The vehicle model used to synthesize the ASR controls is represented by the Bond Graph model (Fig. 3). It is based on the "bicycle" model (Fig. 2) that only considers the rotating rear wheel dynamic and the longitudinal movement.

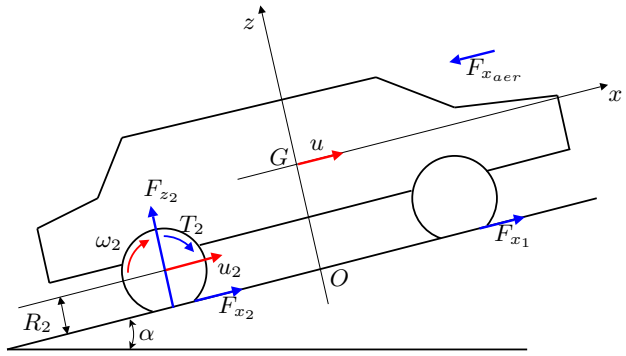


Fig. 2. Vehicle model sketch

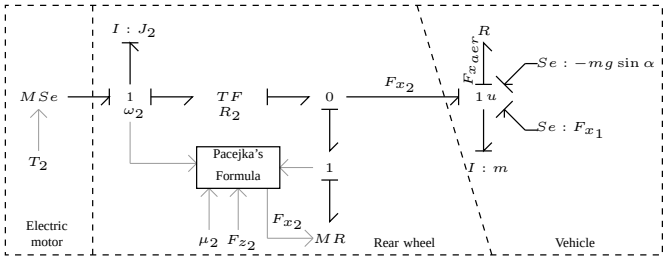


Fig. 3. Bond Graph model for control synthesis

The Bond Graph representation of the vehicle given in Fig. 3 is described by the following nonlinear two states equations model (1).

$$\begin{cases} m\dot{u} = F_{x_1} + F_{x_2}(u, \omega_2, F_{z_2}, \mu_2) - F_{x_{aer}}(u) - mg\sin\alpha \\ J_2\dot{\omega}_2 = T_2 - R_2 F_{x_2}(u, \omega_2, F_{z_2}, \mu_2) \end{cases} \tag{1}$$

B. Linearizing Feedback Synthesis

During acceleration phases, the ASR function aims to maintain the rear wheels slip λ_2 (2) less than a constant value $\lambda_2^\star$. By differentiating (2), [9] bring up the rear wheel slipping λ_2 in the vehicle model (1).

$$\lambda_2 = \frac{R_2\omega_2 - u}{R_2\omega_2} \tag{2}$$

$$\dot{\lambda}_2 = -\frac{\dot{u}}{R_2\omega_2} + \frac{u\dot{\omega}_2}{R_2\omega_2^2} \tag{3}$$

$$\begin{cases} m\dot{u} = F_{x_1} + F_{x_2}(u, \omega_2, F_{z_2}, \mu_2) - F_{x_{aer}}(u) - mg\sin\alpha \\ \dot{\lambda}_2 = \dfrac{u}{J_2R_2\omega_2^2}T_2 - \dfrac{1}{R_2\omega_2}\dot{u} - \dfrac{u}{J_2\omega_2^2}F_{x_2}(u, \omega_2, F_{z_2}, \mu_2) \end{cases} \tag{4}$$

The front wheel-road contact force F_{x_1} and the influence of the slope are considered as perturbations. The evolution of the slipping λ_2 needs to be controlled by means of rear wheel torque T_2. The system (4) has a relative degree of 1 with respect to the output $y = \lambda_2$. Therefore, a new control input U defined by $\frac{d}{dt}(\lambda_2 - \lambda_2^\star) = \dot{\lambda}_2 = U$ is added to transform the vehicle model. $\lambda_2^\star$ is considered to be constant for the control law synthesis.

$$\begin{cases} m\dot{u} = F_{x_1} + F_{x_2}(u, \omega_2, F_{z_2}, \mu_2) - F_{x_{aer}}(u) - mg\sin\alpha \\ \dot{\lambda}_2 = U \end{cases} \tag{5}$$

The driving torque $T_{2_{ASR}}$, which compensates all nonlinear terms and satisfies (5), is defined by the equation (6).

$$T_{2_{ASR}} = \frac{J_2\omega_2}{u}\dot{u} + R_2F_{x_2}(u, \omega_2, F_{z_2}, \mu_2) + \frac{J_2R_2\omega_2^2}{u}U \tag{6}$$

A PI-type stabilizing feedback is chosen for U such that λ_2 converges to $\lambda_2^\star$ (5).

$$U = -k_p\left(\lambda_2 - \lambda_2^\star\right) - k_i\int\left(\lambda_2 - \lambda_2^\star\right)dt \tag{7}$$

An anti-windup system proposed by [10] is added to freeze the integral term when the actuator limits are reached. The linearizing feedback requires the rear wheel velocities and the longitudinal acceleration measurements in order to compute the rear wheel driving torque (6). This controller drives the rear wheels slip λ_2 but not the longitudinal speed of the vehicle. A partial proof of stability is presented in [11] for the residual dynamic u.

C. Flat Control Synthesis

The flat control is a linearizing control law like the other feedback presented in the previous section. In contrary to the controller developed in section II-B, the flat control is a feedforward controller which requires a flat output in order to command all system dynamics. Thus, there is no residual dynamic and the controlled system paired with a stabilizing feedback is exponentially stable outside the singularities.

In [12] a structurally flat output $y_1 = u$ is found on the Bond Graph representation 4 of the vehicle model (1) .

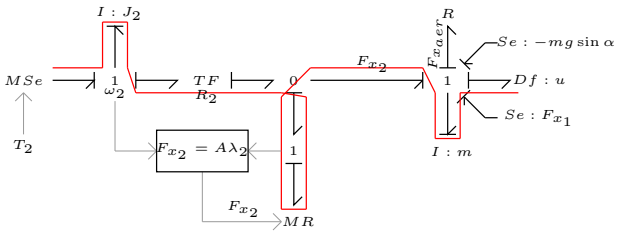


Fig. 4. Structurally flat output

Flat control is an open loop control law. In addition, external disturbances are not predicted. Consequently, the front motor torque T_1, the drag resistance force and the influence of the road slope are neglected during the flat control design. Moreover, when the slipping is low, Pacejka's formula for the longitudinal tire force may be approximated by $F_{x_2} = A\lambda_2$ with A constant (Fig. 5). The vehicle model (1) becomes hence :

$$\begin{cases} m\dot{u} = A\left(1 - \dfrac{u}{R_2\omega_2}\right) \\ J_2\dot{\omega}_2 = T_2 - R_2 A\left(1 - \dfrac{u}{R_2\omega_2}\right) \end{cases} \tag{8}$$

To synthesize the flat control, T_2 must be expressed with respect to the flat output identified on the Bond Graph model and its derivatives. It yields to :

$$y_1 = u \tag{9}$$

$$y_2 = \dot{y}_1 = \frac{A}{m}\left(1 - \frac{u}{R_2\omega_2}\right) \tag{10}$$

$$\begin{aligned} U = y_3 = \ddot{y}_1 &= -\frac{A}{m}\left(\frac{\dot{u}\omega_2 - u\dot{\omega}_2}{R_2\omega_2^2}\right) \\ &= -\frac{A}{m}\frac{\dot{u}}{R_2\omega_2} + \frac{A}{m}\frac{u\dot{\omega}_2}{R_2\omega_2^2} \end{aligned} \tag{11}$$

$$T_2 = \frac{mJ_2y_1U}{AR_2\left(1 - \dfrac{m}{A}y_2\right)^2} + \frac{J_2y_2}{R_2\left(1 - \dfrac{m}{A}y_2\right)} + R_2my_2 \tag{12}$$

The flat controller is not defined when $A = 0$ or $A = my_2$. The wheel is always supposed in contact with the road and the adherence of the road is supposed never null so, the controller is only not defined when $u = 0$. When this specific case occurs, the vehicle's speed is set to a low value close to 0.

As the flatness based controller drives the two dynamics of the system (u, ω_2), it can be assumed that the desired outputs are faithfully followed. In consequence, measured values can be considered equivalent to desired values in absence of perturbations. The driving torque T_2 may be expressed completely with respect to desired values denoted $y_i^\star$.

$$T_2^\star = \frac{mJ_2y_1^\star U^\star}{A^\star R_2\left(1 - \dfrac{m}{A^\star}y_2^\star\right)^2} + \frac{J_2y_2^\star}{R_2\left(1 - \dfrac{m}{A^\star}y_2^\star\right)} + R_2my_2^\star \tag{13}$$

The coefficient $A^\star$, such that $F_{x_2}^\star = A^\star\lambda_2^\star$, is needed to compute the torque T_2 (13) and its value is computed in real time using Pacejka's representation (Fig. 5) for a given constant adherence coefficient of the road and a vertical force to the wheel (14).

$$A^\star = \frac{F_{x_2}^\star\left(\lambda_2^\star, \mu_0, F_{z_0}\right)}{\lambda_2^\star} = \frac{\phi(\lambda_2^\star)\mu_0F_{z_0}}{\lambda_2^\star} \tag{14}$$

The ASR control generally tries to keep as low as possible the slip value λ_2. In consequence, requirements expressed originally for $\lambda_2^\star$ needs to be translated, ie the trajectories of $y_1^\star$, and its derivatives $y_2^\star$ and $y_3^\star$ must be computed from $\lambda_2^\star(u)$. When the slipping is greater (less) than the desired value, the acceleration of the vehicle needs to be reduced (increased). As $y_3^\star$ is $y_2^\star$ derivative it is also $\dot{u}$ derivative. This represents the time derivative of the acceleration (jerk). Therefore, for the ASR function, $y_3^\star$ could be a function of the slipping error e_{λ_2}. $y_3^\star$ is integrated to compute $y_1^\star$ and $y_2^\star$ as shown in equations (16) and (15).

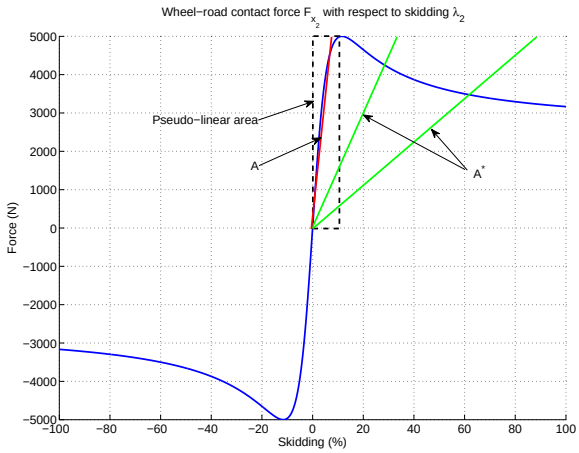


Fig. 5. Pseudo-linear area of Pacejka's representation

$$y_3^\star = K_{y_3}e_{\lambda_2} \qquad K_{y_3} > 0 \tag{15}$$

$$y_2^\star = \int y_3^\star dt \qquad y_2^\star(t_0) = y_2(t_0) \tag{16}$$

$$y_1^\star = \int y_2^\star dt \qquad y_1^\star(t_0) = y_1(t_0) \tag{17}$$

When the open-loop control (13) is applied, the system is equivalent to a double integrator. To ensure stability, a PI error feedback defined from the slipping error e_{λ_2} (19) is applied to $U^\star = y_3^\star$. The close loop system is exponentially stable outside the singularity $u = 0$. Fig. 6 represents the final controller architecture.

$$T_2 = \frac{mJ_2y_1^\star U}{A^\star R_2\left(1 - \dfrac{m}{A^\star}y_2^\star\right)^2} + \frac{J_2y_2^\star}{R_2\left(1 - \dfrac{m}{A^\star}y_2^\star\right)} + R_2my_2^\star \tag{18}$$

$$U = y_3^\star + K_pe_{\lambda_2} + K_i\int e_{\lambda_2}dt \tag{19}$$

$$e_{\lambda_2} = \lambda_2^\star - \lambda_2 \tag{20}$$

III. EXPERIMENTAL VALIDATION

The vehicle has naturally four wheels however the control synthesis model considers only two. A possible approach to overcome this problem is to use 2 "bicycle" models, one for the left side of the vehicle and one for the right side. With this, each side of the vehicle has its own controller. The control laws synthesized in section II have been validated on the VELROUE prototype vehicle equipped with a MABX[4].

[4]MicroAutoBox, dSPACE equipment

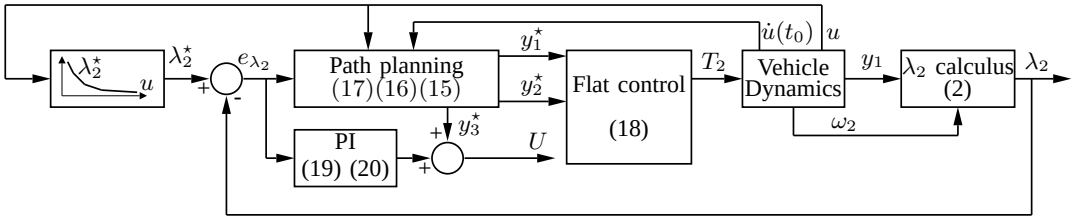


Fig. 6. Flat controller sketch

Electric motors torques, longitudinal acceleration, wheels speed and vehicle speed are measured.

In the chosen validation scenario, the vehicle is driven on a flat road with asymmetric adherence. On the left, the vehicle drives on wet tiles of constant adherence coefficient 0.2. On the right, the coefficient varies from 0.2 to 0.7 thanks to an alternation of wet tiles and wet road. The test corresponds to an electric start up with full acceleration demand during approximatively 7 seconds followed by an acceleration release which causes an energy recovery, then an acceleration and another acceleration release. This scenario is used to study the influence of a variable and asymmetric estimation error of the adherence coefficient (the adherence coefficient is considered constant and of average value in the control law synthesis). The desired slipping $\lambda^\star$ varies slowly according to the vehicle's speed.

The linearizing feedback (6) and the flat controller (18) are compared to a PI controller usually used in the automotive industry. Fig. 7, 8 and 9 illustrates respectively PI controller, linearizing feedback and flat controller experimental results for the test previously described. The Fig. 7 (a), 8 (a) and 9 (a) show the left and right wheels linear velocities in continuous and dashed lines and the vehicle speed in dotted line. The slipping error Fig. (b) correspond to the difference between the measured and desired slipping. The left wheel is plotted in continuous line and the right wheel in dashed line. Fig. (c) and (d) illustrate left and right wheel torques. The motor torque asked by the driver is drawn in a continuous line while the torque computed by the ASR control law is plotted in a dashed line and the measured motor torque is in a dotted line.

At the beginning of each test when the vehicle speed is approximately zero, the rear wheels slipping error varies mainly due to noise on wheels and vehicle speeds measures. On Fig. 7 (PI controller results), when the left wheel begins to slip at 5 seconds, only the left wheel torque is quickly decreased to slow down the left wheel. The wet tiles have no gradualness so, the wheel spins quickly. The torque is then slowly increased to avoid jerks due to fast activation/deactivation of ASR. Meanwhile, the right wheel on the wet road transmits all the torque asked by the driver. Then, when the wheel is on the wet tiles, it starts to slip so, the ASR limits the right motor torque to reduce the slipping. The linearizing feedback (6) reduces correctly the rear wheels slipping error (Fig. 8). The first limitation of torque by the ASR let the wheel slip a little more than following applied torque command, for example on the right wheel at 4 and 12 seconds. This extra slipping is caused by a slower response time due to F_{x_2} estimation error rejection. The same phenomenon appears on the flat control results on Fig. 9 because of the estimation error of A. At 3 and 12s for the left wheel and 5 and 12s for the right wheel, the slipping error increases up to 80%. Then, when the wheels slip again, the slipping error is limited to 20% or 40%. The amplitude of torque limitation is here smaller than for the others control laws torque requests thanks to a better computing of the maximum transmissible torque. Because of higher and closer slipping error peaks, the wheels slipping control of the linearizing feedback is less effective than with the flat controller. Table I summarizes the advantages (+) and drawbacks (-) of each controller according to the performance, the complexity in terms of synthesis and implementation, and the experimental tuning difficulties.

TABLE I

ASR CONTROL LAWS COMPARISON

Control Law	Performance	Complexity	Tuning
PI	-	++	++
Feedback Linearization	- (+)[5]	+	+
Flat Control	+ (++)[5]	-	-

IV. CONCLUSIONS AND FUTURE WORKS

In this paper a linearizing feedback and a flat nonlinear control were synthesized and tested on the VELROUE prototype vehicle. These ASR functions enable the control of each rear wheel independently. Controllers presented in this paper drive properly rear wheels slipping except at the first slipping occurrence where the estimation errors needs to be rejected. The linearizing feedback is less effective than the flat controller, leading to higher and closer slipping error peaks. Future works concerning the improvement of the estimation accuracy of F_{x_2} and A will now be carried out as well as the simplification of the flat controller experimental tuning. MSR[6] which is ASR counterpart for regenerative torque control will also be studied.

V. ACKNOWLEDGMENTS

The authors gratefully acknowledge MICHELIN and IFP, which are RENAULT partners in VELROUE project subsidized by the French Environment and Energy Management Agency.

[5] If the estimation error is minimized

[6] Motor-Schleppmoment-Regelung

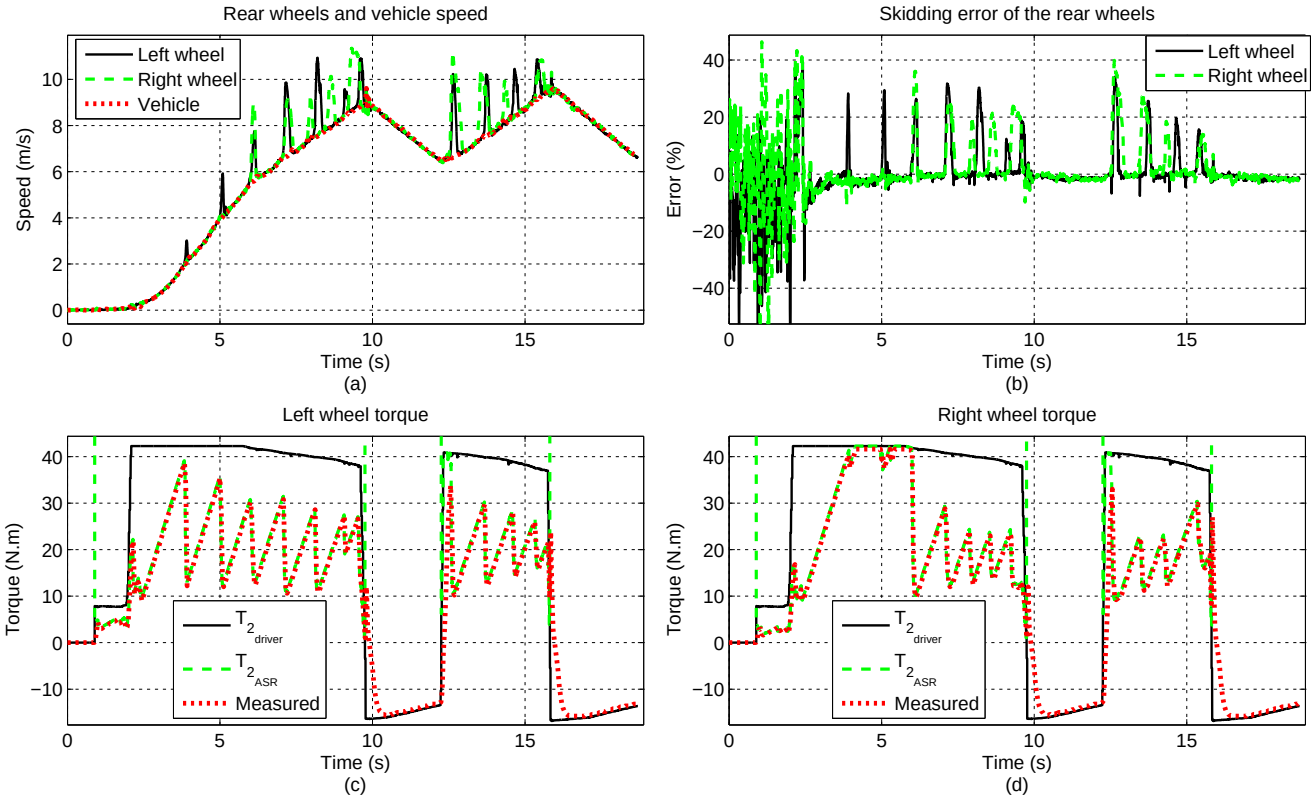


Fig. 7. PI controller experimental results

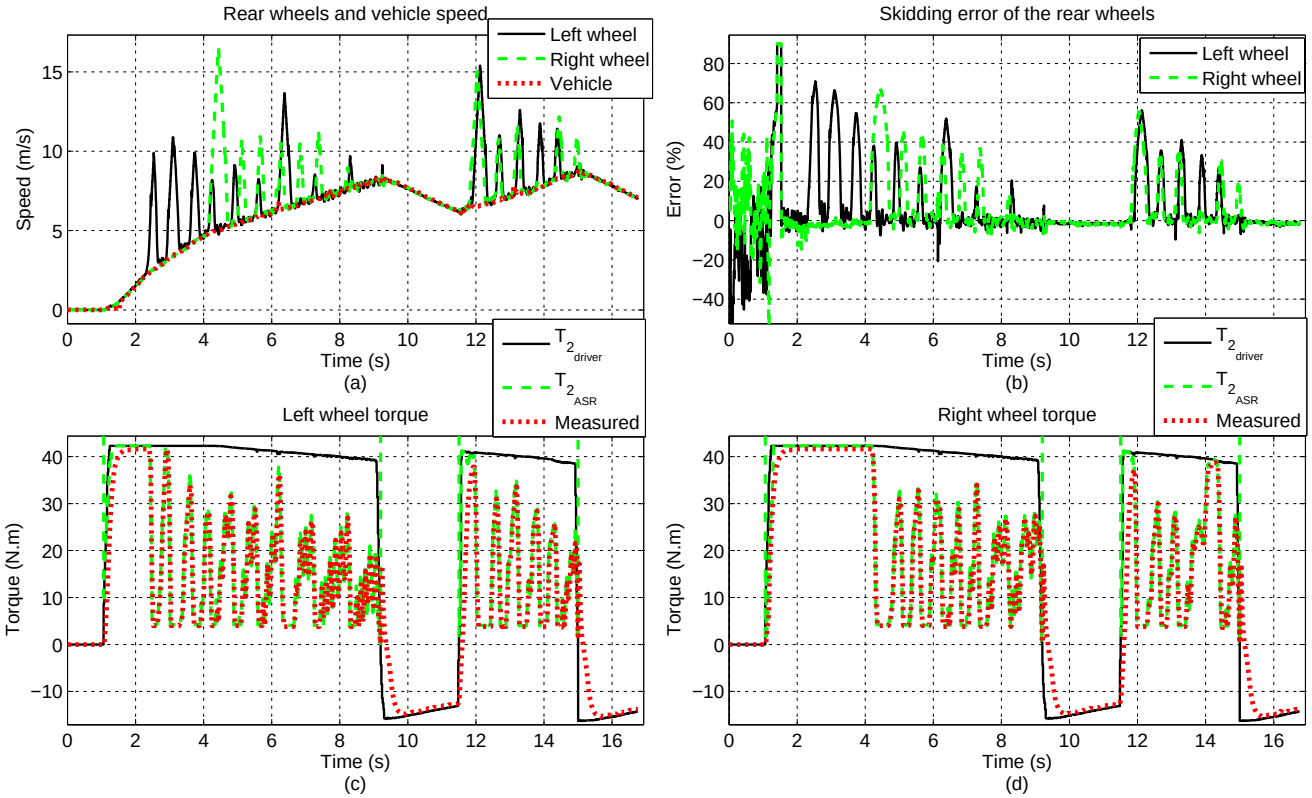


Fig. 8. Linearizing feedback experimental results

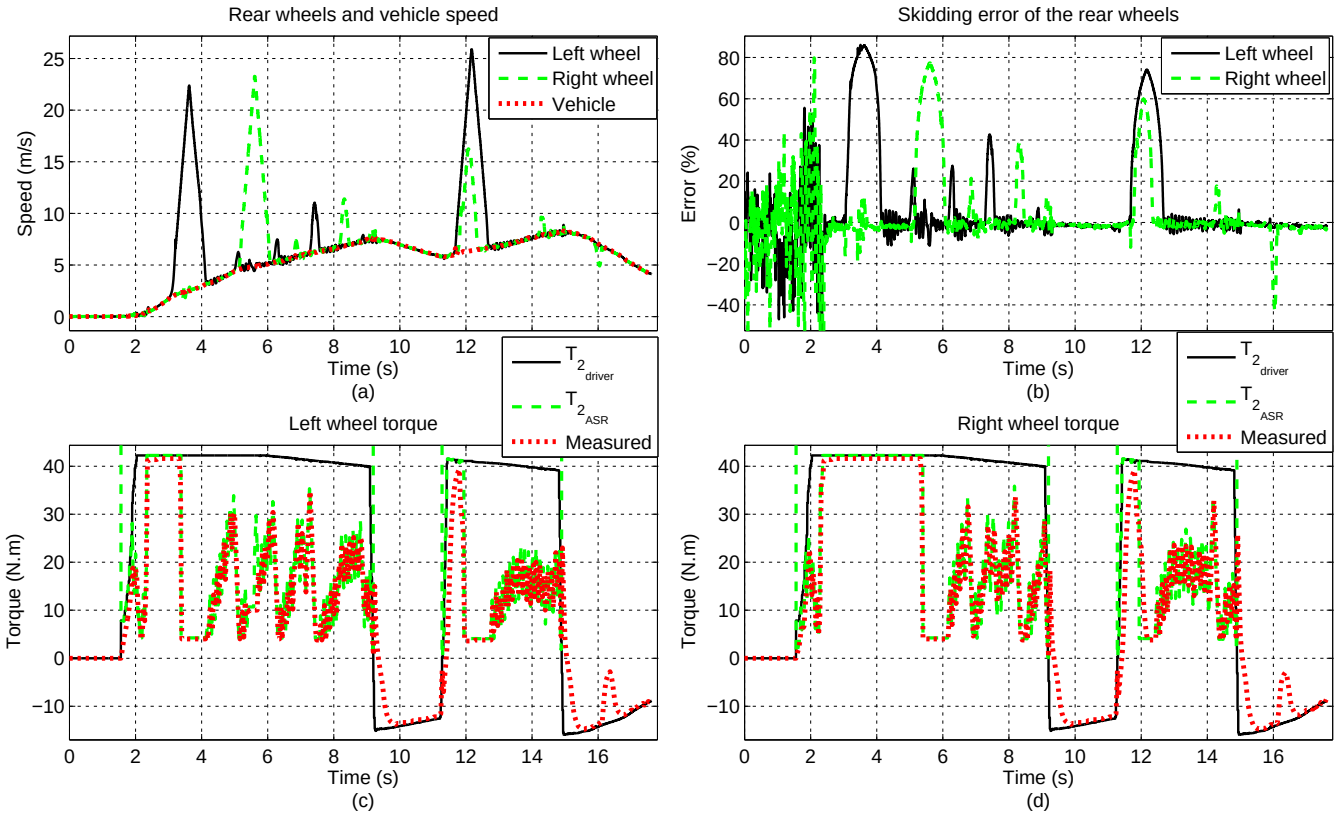


Fig. 9. Flat controller experimental results

REFERENCES

[1] J. Wang, Q. Wang, L. Jin and C. Song, Independent wheel torque control of 4WD electric vehicle for differential drive assisted steering, *Mechatronics*, 2011, Vol. 21, pp.63-76

[2] S. Sakai and Y. Hori, Advantage of Electric Motor for Anti Skid Control of Electric Vehicle, 2000

[3] D. Yin, S. Oh and Y. Hori, A Novel Traction Control for EV Based on Maximum Transmissible Torque Estimation, *IEEE Trans. On Industrial Electronics*, 2009, Vol. 56, No. 6, pp.2086-2094

[4] Z. Fan, Y. Koren and D. Wehe, A Simple Traction Control for Tracked Vehicle, *Proc. of the ACC*, 1995, Vol. 2, pp.1176-1177

[5] C. Canudas and P. Tsiotras, Dynamic Tire Friction Models for Vehicle Traction Control, *Proc. of the IEEE CDC*, 1999, Vol. 4, pp.3746-3751

[6] K. Nam and Y. Hori, Sliding mode controller design for optimal slip control of electric vehicles based on fuzzy vehicle velocity estimation logic, *FISITA*, 2010

[7] C. Canudas, H. Olsson, K. J. Astrm and P. Lischinsky, A new model for control of systems with friction, *IEEE Trans. On Automatic Control*, 1995, pp.419-425

[8] F. Chen and T. Liao, Nonlinear linearization controller and genetic algorithm-based fuzzy logic controller for ABS systems and their comparison, *Int. Journal of Vehicle Design*, 2000, Vol. 4, pp.334-349

[9] T. Nakakuki, T. Shen and K. Tamura, Adaptive control approach to uncertain longitudinal tire slip in traction control of vehicles, *Asian Journal of Control*, 2008, Vol. 10, No. 1, pp.67-73

[10] A. Visioli, Modified anti-windup scheme for PID controllers, *IEE Proc. Control Theory and Applications*, 2003, Vol. 150, pp.49-54

[11] C. Chapuis, N. Minoiu-Enache, X. Brun and E. Bideaux, Controle de l'anti-patinage d'un vehicule electrique par retour linearisant, *CIFA*, 2012

[12] C. Chapuis, X. Brun, E. Bideaux and N. Minoiu-Enache, Anti-Skid Regulation (ASR) of an Electric Vehicle Using Flatness Control, *submitted to AVEC*, 2012

TABLE II

LIST OF SYMBOLS

e_{λ_2}	rear slipping error
g	acceleration of gravity ($m.s^{-2}$)
m	mass (kg)
u	component of the velocity along x ($m.s$)
A	approximation of Pacejka's representation for low values of λ_2 (N)
$A^\star$	real time approximation of Pacejka's representation (N)
$F_{x_{aer}}$	air resistance force (N)
F_{x_1}	front wheel-road contact force (N)
F_{x_2}	rear wheel-road contact force (N)
F_{z_2}	vertical force on the rear wheel (N)
F_{z_0}	constant vertical force used to compute $A^\star$ (N)
J_2	mass moment of inertia of the rear wheel ($kg.m^2$)
K_i	stabilizing loop integral gain
K_p	stabilizing loop proportional gain
K_{y_3}	proportional gain used to plan y_3 path
R_2	radius of the rear wheel (m)
T_2	rear motor torque (Nm)
$T_{2_{ASR}}$	rear motor torque requested by ASR (Nm)
$T_{2_{driver}}$	rear motor torque requested by the driver (Nm)
α	grade angle of the road (rad)
λ_2	slipping of the rear wheel ($\%$)
$\lambda_2^\star$	desired slipping of the rear wheel ($\%$)
μ_0	constant adherence coefficient used to compute $A^\star$
μ_2	adherence coefficient near the rear wheel
ω_2	angular velocity of the rear wheel ($rad.s^{-1}$)
$\phi(\cdot)$	normalized Pacejka's representation